

Nonasymptotic Transport Properties in Fluids and Mixtures Near a Critical Point¹

R. Folk^{2, 3} and G. Moser⁴

We review the critical dynamics of fluids and mixtures. Special attention in the comparison with experiment is paid to nonasymptotic effects. Our theoretical results are based on the complete model H' of Siggia, Halperin, and Hohenberg including the sound mode variables. Using the dynamic renormalization group theory, we calculate the temperature dependence of the transport coefficients as well as the frequency-dependent sound velocity and sound attenuation. In mixtures a time ratio between the Onsager coefficients related to the diffusive modes, which is directly related to the critical enhancement of the thermal conductivity near a consolute point, has to be taken into account. The sound mode contains, besides the dynamic parameters, a static coupling related to the logarithmic derivative of the weakly diverging specific heat. The deviation from the asymptotic value of this coupling at finite frequencies and temperature distance from T_c leads to additional nonasymptotic effects. Our theory, which derives the phenomenological ansatz of Ferrell and Bhattacharjee for pure fluids and mixtures near a consolute point, is also applicable near a plait point.

KEY WORDS: consolute point; dynamic critical phenomena; gas-liquid critical point; mixtures; plait point; renormalization-group theory; sound attenuation; transport properties.

1. INTRODUCTION

Universality of the dynamics at liquid and mixture second-order phase transitions can be proven by measuring the asymptotic values of exponents and amplitude ratios of transport coefficients (TCs) calculated by renormalization group theory (RGT). In order to extract reliable values for

¹ Invited paper presented at the Thirteenth Symposium on Thermophysical Properties, June 22–27, 1997, Boulder, Colorado, U.S.A.

² Institute for Theoretical Physics, University of Linz, Austria.

³ To whom correspondence should be addressed.

⁴ Institute for Physics and Biophysics, University of Salzburg, Austria.

these quantities, it is necessary to include corrections to scaling in the analysis of the experimental data (for a review, see Ref. 1). This was interesting in itself since the correction amplitudes are also related by universal ratios.

However, it has become clear that, although the mixtures lie in the same universality class as the pure fluids, the nonasymptotic corrections are different. It turned out that, in mixtures, an additional dynamic parameter [a combination of Onsager coefficients (OCs)] with a dynamical transient exponent smaller than that of the pure liquid has to be taken into account [2]. This additional parameter allows an understanding of the enhancement of the thermal conductivity, which stays finite near a consolute point and which was observed in a 2-butoxyethanol–water mixture [3].

On the other hand, the behavior of the thermal conductivity near a plait point (vapor–liquid critical point in a mixture) is quantitatively different. In ^3He – ^4He mixtures the thermal conductivity seems to diverge as in the pure liquid [4] (in fact it does not reach its finite asymptotic value within the experimental region), whereas in methane–ethane mixtures, the enhancement could be measured [5] recently. However, the enhancement is much larger than that at the consolute point. This could be understood by the different choice of the order parameter at a consolute point and the plait point [6].

The description of the crossover from the background region (with regular nonuniversal behavior) to the asymptotic region (with universal power law behavior) requires the calculation of crossover functions which could be checked by comparison with experiment. Most of such calculations were performed within mode coupling theory (MCT) [7] (for a review, see Ref. 8). Here we present the results for such crossover functions obtained within RGT and a more complete analysis of the experimental results [1]. In particular, a nonasymptotic RGT of models H and H' [9] has been formulated in Ref. 2 and compared with experiments at the vapor–liquid critical point in pure fluids, as well as at the consolute point [10] and at the plait point [6] in mixtures.

Within RGT the nonasymptotic behavior can be understood as a crossover of the model's (static or dynamic) coupling parameters from their background values to their fixed point values at T_c . The dependence of the model coupling parameters is calculated by RGT and inserted in the crossover functions to be considered, e.g., for the TCs. Such an approach had been developed for the critical dynamics near the superfluid transition [11] and applies here equally well.

A further application of RGT is the calculation of critical effects in sound propagation. This is achieved by including the longitudinal dynamical

degrees of freedom into the set of dynamical model equations. Recently we performed such a calculation near the pure liquid critical point [10, 12], here we consider the more complicated situation in mixtures. For pure liquids and for the consolute point, a phenomenological theory was developed in Refs. 13 and 14. For pure fluids a basis for the phenomenological theory was given in Ref. 15 by the extension of model H, and in Refs. 10, 12, and 16, a nonasymptotic RGT was formulated and compared with experiments (for a recent asymptotic calculation, see Ref. 17). So far, no theoretical basis by RGT was presented for the consolute point and no theoretical results were available for the plait point [18]. Our nonasymptotic results for the critical sound propagation in all cases involve, besides thermodynamic quantities, the dynamic parameters determined from other TCs. The static coupling constant of the sound degrees of freedom to the order parameter is found to be the logarithmic derivative of an appropriate weakly diverging compressibility in all cases and has the property to decrease to zero approaching the background.

2. CRITICAL DYNAMICS OF MIXTURES

2.1. The Model Equations

The critical dynamics of a mixture is described by the equations of motion for the entropy densities $\sigma(x)$, the local concentration $c(x)$, and the transverse momentum current $\mathbf{j}_\perp(x)$. If the sound propagation should also be described, we have to add the equations for the mass density $\rho(x)$ and the longitudinal momentum current $\mathbf{j}_\parallel(x)$. At the consolute point the local concentration constitutes the order parameter density and we choose as densities ϕ , q_1 , and q_2 as the linear combination of the fluctuations $\Delta c(x)$, $\Delta\sigma(x)$, and $\Delta\rho(x)$,

$$\begin{aligned}\phi(x) &= \sqrt{N_A} (\Delta c(x) - \langle \Delta c(x) \rangle) \\ q_1(x) &= \sqrt{N_A} \left[\Delta\sigma(x) - \left(\frac{\partial\sigma}{\partial c} \right)_{T,P} (\Delta c(x) - \langle \Delta c(x) \rangle) \right] \\ q_2(x) &= \sqrt{N_A} \left[\Delta\rho(x) - \left(\frac{\partial\rho}{\partial c} \right)_{T,P} (\Delta c(x) - \langle \Delta c(x) \rangle) \right]\end{aligned}\quad (1)$$

whereas at the plait point and at the critical point in pure fluids, the entropy density constitutes the order parameter and the densities read accordingly,

$$\begin{aligned}
\phi(x) &= \sqrt{N_A} (\Delta\sigma(x) - \langle \Delta\sigma(x) \rangle) \\
q_1(x) &= \sqrt{N_A} \left[\Delta c(x) - \left(\frac{\partial c}{\partial \sigma} \right)_{A,P} (\Delta\sigma(x) - \langle \Delta\sigma(x) \rangle) \right] \\
q_2(x) &= \sqrt{N_A} \left[\Delta\rho(x) - \left(\frac{\partial \rho}{\partial \sigma} \right)_{A,P} (\Delta\sigma(x) - \langle \Delta\sigma(x) \rangle) \right]
\end{aligned} \tag{2}$$

q_1 terms are to be skipped for pure fluids. Statics is described by the Hamiltonian

$$\begin{aligned}
H = \int d^d x \frac{1}{2} \left\{ \tau \phi^2(x) + (\nabla\phi(x))^2 + a_{11} q_1^2(x) + a_{22} q_2^2(x) + 2a_{12} q_1(x) q_2(x) \right. \\
+ a_j \mathbf{j}^2(x) + \frac{\tilde{u}}{12} \phi^4(x) + \gamma_1 q_1(x) \phi^2(x) \\
\left. + \gamma_2 q_2(x) \phi^2(x) - 2h_1 q_1(x) - 2h_2 q_2(x) \right\}
\end{aligned} \tag{3}$$

leading to strongly and weakly diverging thermodynamic derivatives (the $a_{i,j}$ are thermodynamic background values), which are, in the case of the consolute point,

$$\langle \phi \phi \rangle_c = \frac{RT}{\rho} \left(\frac{\partial c}{\partial \Delta} \right)_{T,P}, \quad \langle q_1 q_1 \rangle_c = \frac{RT}{\rho} \left(\frac{\partial \sigma}{\partial T} \right)_{c,P} \tag{4}$$

$$\langle q_2 q_2 \rangle_c = RT\rho \left(\frac{\partial \rho}{\partial P} \right)_{T,c}, \quad \langle q_1 q_2 \rangle_c = RT\rho \left(\frac{\partial \sigma}{\partial P} \right)_{T,c} = \frac{RT}{\rho} \left(\frac{\partial \rho}{\partial T} \right)_{c,P} \tag{5}$$

and, in the case of a plait point,

$$\langle \phi \phi \rangle_c = \frac{RT}{\rho} \left(\frac{\partial \sigma}{\partial T} \right)_{A,P}, \quad \langle q_1 q_1 \rangle_c = \frac{RT}{\rho} \left(\frac{\partial c}{\partial \Delta} \right)_{\sigma,P} \tag{6}$$

$$\langle q_2 q_2 \rangle_c = RT\rho \left(\frac{\partial \rho}{\partial P} \right)_{\sigma,A}, \quad \langle q_1 q_2 \rangle_c = RT\rho \left(\frac{\partial c}{\partial P} \right)_{\sigma,A} = \frac{RT}{\rho} \left(\frac{\partial \rho}{\partial \Delta} \right)_{\sigma,P} \tag{7}$$

The appropriate dynamic equations are an extension of model H' [9, 2]:

$$\frac{\partial \phi}{\partial t} = \Gamma \nabla^2 \frac{\delta H}{\delta \phi} + L \nabla^2 \frac{\delta H}{\delta q_1} + L_\phi \nabla^2 \frac{\delta H}{\delta q_2} - g(\nabla \phi) \frac{\delta H}{\delta \mathbf{j}} + \Theta_\phi \quad (8)$$

$$\frac{\partial q_1}{\partial t} = L \nabla^2 \frac{\delta H}{\delta \phi} + \mu \nabla^2 \frac{\delta H}{\delta q_1} + L_{12} \nabla^2 \frac{\delta H}{\delta q_2} - g(\nabla q_1) \frac{\delta H}{\delta \mathbf{j}} + \Theta_1 \quad (9)$$

$$\begin{aligned} \frac{\partial q_2}{\partial t} = & L_\phi \nabla^2 \frac{\delta H}{\delta \phi} + L_{12} \nabla^2 \frac{\delta H}{\delta q_1} + \lambda \nabla^2 \frac{\delta H}{\delta q_2} - c_2 \nabla \frac{\delta H}{\delta \mathbf{j}} \\ & - g \nabla \left(q_2 \frac{\delta H}{\delta \mathbf{j}} \right) - g_\epsilon \phi \nabla \frac{\delta H}{\delta \mathbf{j}} + \Theta_2 \end{aligned} \quad (10)$$

$$\begin{aligned} \frac{\partial \mathbf{j}_l}{\partial t} = & \lambda_l \nabla^2 \frac{\delta H}{\delta \mathbf{j}_l} - c_2 \nabla \frac{\delta H}{\delta q_2} - g_\epsilon \nabla \left(\phi \frac{\delta H}{\delta q_2} \right) \\ & + (1 - \mathcal{F}) g \left\{ (\nabla \phi) \frac{\delta H}{\delta \phi} + (\nabla q_1) \frac{\delta H}{\delta q_1} - q_2 \nabla \frac{\delta H}{\delta q_2} \right\} \\ & - g(1 - \mathcal{F}) \left\{ \sum_k \left[j_k \nabla \frac{\delta H}{\delta j_k} - \nabla_k \mathbf{j} \frac{\delta H}{\delta j_k} \right] \right\} + \Theta_l \end{aligned} \quad (11)$$

$$\begin{aligned} \frac{\partial \mathbf{j}_l}{\partial t} = & \lambda_l \nabla^2 \frac{\delta H}{\delta \mathbf{j}_l} + \mathcal{F} g \left\{ (\nabla \phi) \frac{\delta H}{\delta \phi} + (\nabla q_1) \frac{\delta H}{\delta q_1} - q_2 \nabla \frac{\delta H}{\delta q_2} \right\} \\ & - g \mathcal{F} \left\{ \sum_k \left[j_k \nabla \frac{\delta H}{\delta j_k} - \nabla_k \mathbf{j} \frac{\delta H}{\delta j_k} \right] \right\} + \Theta_l \end{aligned} \quad (12)$$

There are now three model OCs according to the modes of mass diffusion, heat diffusion, and the OCs for the corresponding crossover phenomena. All other OCs in the equation are related to these [2]. The mode couplings g , g_ϵ give rise to critical effects in the OCs and the deviation from van Hove theory. The fluctuating forces Θ_i are Gaussian distributed and fulfill the usual Einstein relations.

We define suitable dynamical parameters, the diffusion rate ratio w and the mode coupling f ,

$$w = \frac{L}{\sqrt{\Gamma \mu}}, \quad f = \frac{g}{\sqrt{\Gamma \lambda_l}} \quad (13)$$

Only these two parameters besides Γ , the order parameter OC, enter the physical expressions for the TCs because irrelevant parameters are neglected. One should note, first, that the physical meaning of the model OCs depends on the definition of the set of variables in Eq. (1) or (2) and,

second, that for the same reason the dynamic parameters enter the TCs in different ways.

2.2. Universality

In order to calculate the dynamical critical effects, we apply RGT to this model. The asymptotic singularities are determined already by the set of equations for ϕ , q_1 , and \mathbf{j}_t alone, and it turns out that they are the same as those obtained in the even simpler model H for the pure fluid [9]. Thus the dynamical critical exponent z is the same as for pure fluids, $z = 4 - x_\lambda - \eta \sim 3$, where the nontrivial exponent x_λ is calculated from the renormalization of the order parameter OC and η is the static critical exponent of the correlations at T_c . This establishes universality at critical points in fluids, although for mixtures an additional dynamical parameter w appears. However, the fixed point value for w is $w^* = 0$ and that of the mode coupling f is the same as found for pure fluids. The transient exponent of w is related by $\omega_w = \frac{1}{2}x_\lambda$ to the pure fluid critical exponent x_λ . The exponent of the shear viscosity is $x_\eta = 1 - x_\lambda - \eta$ in all cases. In consequence, appropriate defined dynamical amplitude ratios, e.g., the Kawasaki amplitude, have the same asymptotic values at the different critical points.

In the nonasymptotic region the model parameters are different from their fixed point values and depend on (i) the distance from the critical point and (ii) the specific fluid considered. The dependence of the parameters on the distance from the critical point is described within RGT by flow equations with the values of the parameters in the background as initial conditions. These have to be found by comparing the theoretical expressions for one or two TCs with experiment.

3. TEMPERATURE DEPENDENCE OF THE TRANSPORT COEFFICIENTS

The expressions of the TCs are obtained by comparing the dispersion of the hydrodynamic modes calculated from the model equations above with those from the hydrodynamic equations for a mixture [19],

$$\begin{aligned} \frac{\partial \sigma}{\partial t} = & \left[\frac{Dk_T}{T} \left(\frac{k_T}{T} \left(\frac{\partial \Delta}{\partial c} \right)_{T,P} - \left(\frac{\partial \Delta}{\partial T} \right)_{c,P} \right) + \frac{\kappa}{\rho T} \right] \nabla^2 T \\ & + D \left[\frac{k_T}{T} \left(\frac{\partial \Delta}{\partial c} \right)_{T,P} - \left(\frac{\partial \Delta}{\partial T} \right)_{c,P} \right] \nabla^2 c \end{aligned} \quad (14)$$

$$\frac{\partial c}{\partial t} = \frac{Dk_T}{T} \nabla^2 T + D \nabla^2 c, \quad \frac{\partial \mathbf{j}_t}{\partial t} = \frac{\eta}{\rho} \nabla^2 \mathbf{j}_t \quad (15)$$

$$\frac{\partial \rho(x, t)}{\partial t} + \nabla \mathbf{j}'_i(x, t) = 0 \quad (16)$$

$$\frac{\partial \mathbf{j}'_i(x, t)}{\partial t} + \nabla P(x, t) - \frac{1}{\rho} \left(\zeta + \frac{4}{3} \bar{\eta} \right) \nabla (\nabla \mathbf{j}'_i(x, t)) = 0 \quad (17)$$

In this way relations between the model vertex functions and the hydrodynamic TCs are established. The vertex functions are expressed by thermodynamic quantities (the static vertex functions) and the dynamic parameters.

3.1. Mixtures Near a Consolute Point

Let us consider as an example of this procedure a mixture near the consolute point. From the structure of the dynamic model, a nonperturbative relation between the mass diffusion D and the thermal diffusion ratio k_T is obtained. The thermal diffusion ratio is *exactly* the inverse of the mass diffusion over the whole temperature region from asymptotics to the background (R here is the gas constant)

$$k_T(t) = \frac{\rho L}{RD(t)} \quad (18)$$

This has been verified in Ref. 20 for aniline–cyclohexane up to values of $t \sim 10^{-2}$, but it would be worthwhile to prove this for larger values of t . In passing we mention that such a simple exact relation does not hold near plait points. There, it is fulfilled only in the asymptotic region [2].

Inserting for the vertex functions calculated in one loop order, we obtain the final results for the TCs, namely, the mass diffusion,

$$D(t) = \xi(t)^{-2} \Gamma(t) \left(1 - \frac{1}{16} f^2(t) \right) \quad (19)$$

the shear viscosity,

$$\bar{\eta}(t) = \frac{k_B T}{4\pi} \xi(t) \left[\left(1 - \frac{1}{36} \frac{f^2(t)}{1 - w^2(t)} \right) / \Gamma(t) f^2(t) \right] \quad (20)$$

and the thermal conductivity,

$$\frac{\kappa(t)}{\rho T} = \frac{\rho}{RT} \mu \left(1 - \frac{w^2(t)}{1 - \frac{1}{16} f^2(t)} \right) \quad (21)$$

with

$$\begin{aligned} \frac{d\Gamma}{dt} &= \frac{d \ln \xi(t)}{dt} \frac{3}{4} \Gamma f^2, & \frac{dw}{dt} &= -\frac{d \ln \xi(t)}{dt} \frac{3}{8} w f^2 \\ \frac{df}{dt} &= \frac{d \ln \xi(t)}{dt} \frac{1}{2} f \left(1 - \frac{3}{4} f^2 - \frac{1}{24} \frac{f^2}{1-w^2} \right) \end{aligned} \quad (22)$$

Thus the critical enhancement of the thermal conductivity is directly related to the temperature dependence of the parameter $w(t)$.

The general procedure is now to determine the initial parameters of the flow equations [Eq. (22)] by comparing with one or two TCs in a certain temperature region. We use the shear viscosity [Eq. (20)], but one has to keep in mind that the thermal conductivity [Eq. (21)] is most sensitive

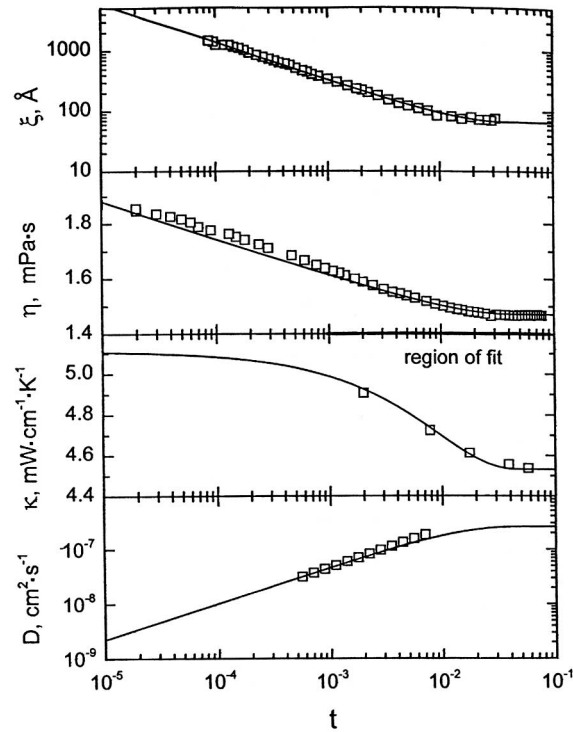


Fig. 1. Comparison of theory with 2-butoxyethanol-water data (see text for the Refs.). Fit of the correlation length ξ of the shear viscosity η , the thermal conductivity κ , and our prediction for the mass diffusivity D compared with the experimental data.

to the flow of w and would be the most sensitive experimental quantity to be fitted in order to find $w(t_0)$. Unfortunately, no such data are usually available, and therefore, the shear viscosity serves for the determination of all three initial parameters $\Gamma(t_0)$, $f(t_0)$, and $w(t_0)$.

The mixture 2-butoxyethanol–water is an exceptional case. First, the correlation length data extend into the background region and all three TCs have been measured [3, 21]. We have performed fits of the shear viscosity corrected for the regular temperature behavior. For the background the uncorrected shear viscosity is increasing since we approach T_c from below. The corrected data lead to a nonzero background value of the parameter w . This indicates and, assuming this value of w is valid, predicts a critical enhancement of the thermal conductivity. Here we include the experimentally observed enhancement in our fit procedure and then predict

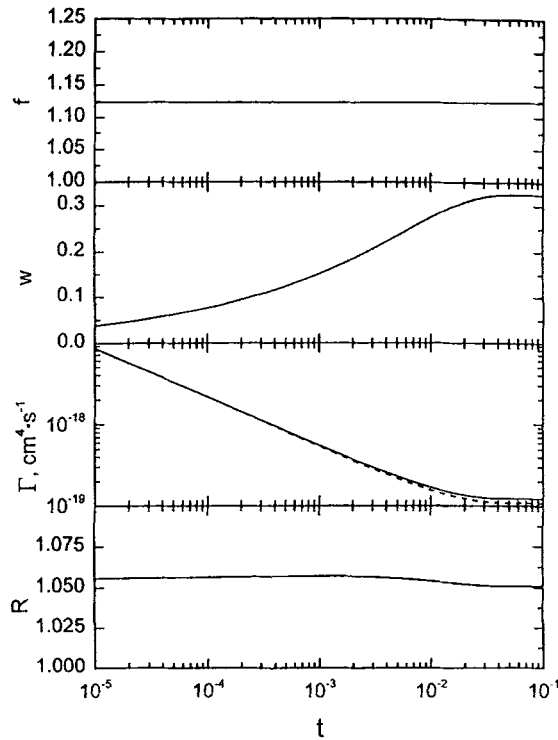


Fig. 2. Dynamic parameters f and w , Onsager coefficients Γ (solid curve), Γ_{eff} (dashed curve), and Kawasaki amplitude R for 2-butoxyethanol–water as a function of the temperature distance t from T_c .

the mass diffusion (see Figs. 1 and 2); aniline–cyclohexane has been analyzed in Refs. 10 and 22.

3.2. Nonuniversal Kawasaki Amplitude

The experimentally defined Kawasaki amplitudes [7] at the consolute point and for pure fluids read

$$R_{\text{exp}}^{\text{cons}} = \frac{6\pi\eta D_T \xi}{k_B T} \quad \text{and} \quad R_{\text{exp}}^{\text{pure}} = \frac{6\pi\eta D_T \xi}{k_B T} \quad (23)$$

respectively. A more complicated expression applies for the plait point [2]. Inserting the theoretical expressions, we obtain the nonasymptotic amplitude ($w \equiv 0$ for pure fluids),

$$R_{\text{th}} = \frac{3}{2f^2(t)} \left(1 - \frac{1}{16} f^2(t)\right) \left(1 - \frac{1}{36} \frac{f^2(t)}{1 - w^2(t)}\right) \quad (24)$$

Although the asymptotic value of the Kawasaki amplitude is $R_{\text{theor}}^* = 1.056$ in all cases, the nonasymptotic expression shows quite different crossover behavior. For the consolute point its value is within 10% of the asymptotic one (see Fig. 2), whereas for the vapor–liquid transitions, it increases to its larger background value (see Figs. 2 and 3 in Ref. 22). This is connected to the different flow of the mode coupling at consolute points (f staying almost at its fixed point value even in the background) and gas–liquid critical points (f decreasing farther away from T_c to its small background value).

4. SOUND MODE

So far only the model H' equations have been considered; now we include the equations for the mass density and the longitudinal momentum current, i.e., consider the whole set, Eqs. (8)–(12). This enables us to calculate the critical effects in the sound velocity c_s and the sound attenuation α_s ,

$$c_s^2(t, \omega) = \Re[\mathcal{C}_s^2(t, \omega) - i\omega\mathcal{D}_s(t, \omega)] \quad \text{and} \\ \alpha_s(t, \omega) = -\frac{\omega \Im[\mathcal{C}_s^2(t, \omega) - i\omega\mathcal{D}_s(t, \omega)]}{2c_s^3(t, \omega)} \quad (25)$$

We neglect the subleading terms \mathcal{D}_s in the following; however, these terms are important in order to reproduce the proper hydrodynamic result in the

background. The structure of \mathcal{C}_s turns out to be the same for all critical points (it agrees also with the formal expressions at the superfluid transition in ${}^4\text{He}$ [23, 24]),

$$\mathcal{C}_s^2(t, \omega) = c_{s1}^2 + c_{s2}^2[\bar{t}] \frac{1 + \gamma^2[\bar{t}] F_+^{(s)}(u[\bar{t}])}{1 + \gamma^2[\bar{t}] F_+(v[t, \bar{t}], w[\bar{t}])} \quad (26)$$

with $\bar{t}(t, \omega)$ found from the matching condition below. The sound velocity at zero frequency reads $c_s^2(t, 0) = c_{s1}^2 + c_{s2}^2$, and only c_{s2}^2 contains the singular part proportional to \bar{t}^α . Straightforward calculations lead for pure fluids to $c_{s1}^2 = 0$ and $c_{s2}^2 = (\partial P / \partial \rho)_\sigma$. For mixtures c_{s1} and c_{s2} , containing T_c -line derivatives, depend on whether we are near a consolute or a plait point. For the consolute point we obtain with $c_{s2}^2 \sim (\partial P / \partial \rho)_{T,c}$ the structure of the ansatz of the phenomenological theory of Ferrell and Bhattacharjee [13, 14] and the scaling properties agree with those mentioned in Ref. 25. For the plait point $c_{s2}^2 \sim (\partial P / \partial \rho)_{\sigma, \Delta}$ (Δ is the difference in chemical potential of the mixture components), and the same asymptotic scaling behavior as at the consolute point is obtained. However, the nonasymptotic behavior might be different.

The static coupling γ between the order parameter and the sound mode degrees of freedom is related to the logarithmic derivatives of the singular part of the sound velocity and may be approximated by

$$\gamma^2(\bar{t}) = \frac{2}{v} \frac{d \ln c_{s2}^2(\bar{t})}{d \ln \bar{t}} \quad (27)$$

In the asymptotic limit it takes its fixed point value, $\gamma^{*2} = 2(\alpha/v)$.

The function F_+ is an amplitude function, related to the so-called ‘‘frequency-dependent specific heat’’ (although we would not use such a name at the plait point, where it is more a concentration susceptibility), which can be calculated within the simpler model H and reads

$$F_+(v, w) = -\frac{1}{4} \left\{ \frac{v^2}{v_+ v_-} \ln v + \frac{1}{v_+ - v_-} \left[\frac{v_-^2}{v_+} \ln v_- - \frac{v_+^2}{v_-} \ln v_+ \right] \right\} \quad (28)$$

with

$$v_\pm = \frac{v}{2} \pm \sqrt{\left(\frac{v}{2}\right)^2 + i\bar{w}} \quad (29)$$

The parameters v and \bar{w} are

$$v[t, \bar{t}] = \frac{\xi^{-2}(t)}{\xi^{-2}[\bar{t}]}, \quad \bar{w}[\bar{t}] = \frac{\omega}{2\Gamma_{\text{eff}}[\bar{t}] \xi^{-4}[\bar{t}]} \quad (30)$$

The temperature distance t and the frequency ω also enter via the effective temperature distance \bar{t} , which is finite at finite frequency in the limit $t=0$ by the matching condition,

$$t^{8\nu} + \left(\frac{2\xi_0^4 \omega}{\Gamma_{\text{eff}}[\bar{t}(t, \omega)]} \right)^2 = \bar{t}^{8\nu}(t, \omega) \tag{31}$$

The effective OC of the order parameter, which appears in the frequency variable $\bar{\omega}$ and the matching condition, contains for the mixtures the dynamic parameter w , $\Gamma_{\text{eff}} = \Gamma(1 - w^2)$. The effect of w is to increase the region of validity of the asymptotic power law behavior of $\Gamma(t)$; see, e.g., the dashed curve in Fig. 2.

4.2. Pure Fluids

At T_c the attenuation in one wavelength, $\alpha_x \times \lambda$, reaches in pure fluids a finite universal value for small frequencies, whereas in mixtures it goes to zero like $\omega^{\alpha/z\nu}$. However, one should be cautious in applying the asymptotic results in the experimental regime because of nonasymptotic effects in the various couplings and/or static quantities involved (see, e.g., for the consolute point [26]). In pure fluids at finite but low frequencies, a nonuniversal value of the attenuation in one wavelength is observed and this value

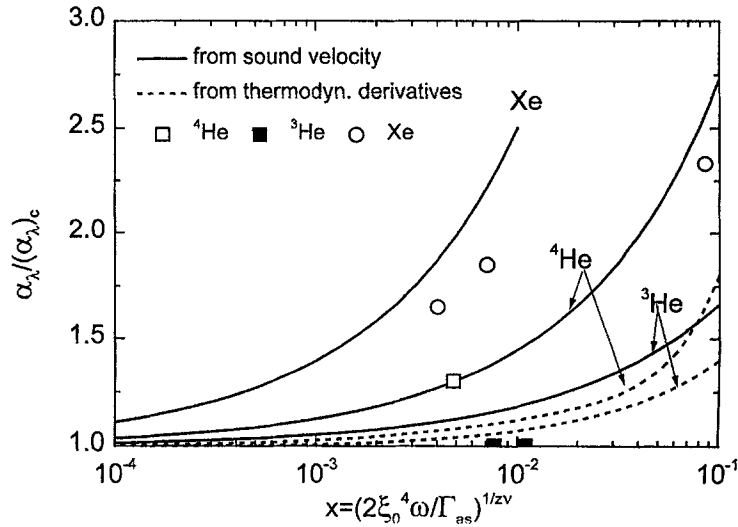


Fig. 3. Normalized attenuation in one wavelength at T_c as function of scaled frequency x .

was related to the nonasymptotic behavior of the specific heat $C_V(t)$ by Bhattacharjee and Ferrell [13]. In our theory this effect is of the same physical origin and related to the nonasymptotic behavior of the static coupling γ^2 shown in Fig. 3. From Eq. (26) we calculate the ratio of the attenuation in one wavelength at finite frequency to the value at zero frequency at T_c

$$\frac{\alpha_\lambda}{(\alpha_\lambda)_c} = \frac{\gamma_q^2(x)}{\gamma_q^{*2}} \frac{1 + (\gamma_q^{*2}/4) \ln 2}{1 + (\gamma_q^2(x)/4) \ln 2} \quad (32)$$

where $x = (2\xi_0^4 \omega / \Gamma_{as})^{1/z\nu}$ is the effective temperature distance at finite frequency. Figure 3 shows our results in comparison with the experimental values given in Ref. 13. Very near T_c (where linearization around the fixed

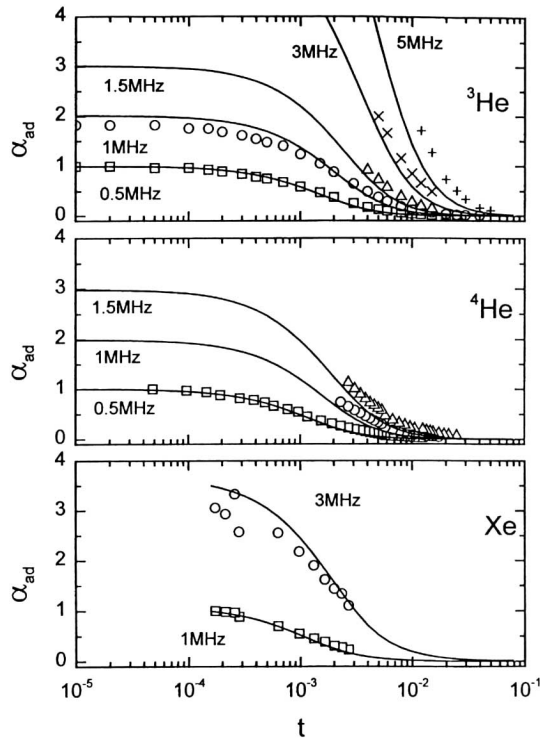


Fig. 4. Adjusted attenuation as a function of the temperature distance from T_c at various frequencies in different liquids. The value of the attenuation is adjusted to one for each liquid at the lowest frequency and smallest temperature distance t from T_c .

point is allowed), the specific heat or compressibility might be fitted by an expression including Wegner corrections to the asymptotic power law, $C_V \sim t^{-\alpha}(1 + gt^A)$, with $A=0.5$. Then, it is seen from the logarithmic derivative of the specific heat that the existence of a maximum in the attenuation in one wavelength depends on the sign of g . For a negative amplitude, a maximum is predicted, whereas for a positive amplitude the attenuation decreases monotonically to zero in the background (high frequencies), when the specific heat reaches its constant positive background value. Thus our result produces the expected [13] behavior in the background region for high frequencies (large x). An extensive comparison of the sound velocity and attenuation for various fluids can be found in Ref. 12. Here we show three examples for the attenuation in ^3He [27], ^4He [28], and Xe [29] in Fig. 4, including all nonasymptotic effects of static and dynamic origin.

ACKNOWLEDGMENT

We thank H. Meyer for valuable discussions and for sending us the experimental data for ^4He and ^3He .

NOTE ADDED IN PROOF

An expression of the same structure as Eq. (26) for the asymptotic regime has been found in an intuitive derivation by A. Onuki (see *J. Phys. Soc. Jpn.* **66**:511 (1997), and this conference). It agrees with our expression in the asymptotic regime concerning the static factors c_{s1}^2 and c_{s2}^2 but differs numerically, as to be expected, in the dynamic part because of different methods of calculation. The differences in the dynamical function are given in a recent paper by A. Kogan and H. Meyer (*J. Low Temp. Phys.*, in press), where a comparison of our nonasymptotic and asymptotic theory as well as the asymptotic theory of Onuki [17] for the pure fluids ^3He and ^4He has been performed. We thank A. Kogan, H. Meyer, and A. Onuki for sending us pre- and/or reprints of their paper.

REFERENCES

1. V. Privman, P. C. Hohenberg, and A. Aharony, in *Phase Transitions and Critical Phenomena*, Vol. 14, C. Domb and J. L. Lebowitz, eds. (Academic Press, New York, 1991).
2. R. Folk and G. Moser, *J. Low Temp. Phys.* **99**:11 (1995).
3. H. Mensah-Brown and W. A. Wakeham, *Int. J. Thermophys.* **16**:237 (1995).
4. L. H. Cohen, M. Dingus, and H. Meyer, *J. Low Temp. Phys.* **49**:545 (1982).
5. E. P. Sankonidou, H. R. van den Berg, C. A. ten Seldam, and J. V. Sengers, *Phys. Rev. E* **56**:R4943 (1997); *J. Chem. Phys.* **109**:717 (1998).

6. R. Folk and G. Moser, *Europhys. Lett.* **24**:533 (1993).
7. K. Kawasaki, *Ann. Phys.* **61**:1 (1970).
8. J. V. Sengers, in *Supercritical Fluids: Fundamentals for Application*, E. Kiran and J. M. H. Levelt Sengers, eds. (Kluwer, Dordrecht, 1994); J. V. Sengers, in *Transport Properties of Fluids: Their Correlation, Prediction and Estimation*, J. Millat, J. H. Dymond, and C. A. Nieto de Castro, eds. (Cambridge University Press, Cambridge, 1996).
9. E. D. Siggia, B. I. Halperin, and P. C. Hohenberg, *Phys. Rev. B* **13**:2110 (1976); C. De Dominicis and L. Peliti, *Phys. Rev. B* **18**:353 (1978).
10. R. Folk and G. Moser, *Phys. Rev. Lett.* **75**:2706 (1995).
11. V. Dohm and R. Folk, *Phys. Rev. Lett.* **46**:349 (1981); V. Dohm, *J. Low. Temp. Phys.* **69**:51 (1987).
12. R. Folk and G. Moser, *Phys. Rev. E* **57**:683, 705 (1998).
13. J. K. Bhattacharjee and R. A. Ferrell, *Phys. Lett. A* **76**:290 (1980); **86**:109 (1981); **88**:77 (1982).
14. R. A. Ferrell and J. K. Bhattacharjee, *Phys. Rev. A* **31**:1788 (1985).
15. R. Dengler and F. Schwabl, *Europhys. Lett.* **4**:1233 (1987).
16. R. Folk and G. Moser, *Proceedings of the RG96-conference*, Dubna, Aug. 1996.
17. A. Onuki, *Phys. Rev. E* **55**:403 (1997).
18. T. Doiron, D. Gestrich, and H. Meyer, *Phys. Rev. B* **22**:3202 (1980).
19. L. D. Landau and E. M. Lifshitz, *Fluid Mechanics*, 2nd ed. (Pergamon, New York, 1987).
20. M. Giglio and A. Vendramini, *Phys. Rev. Lett.* **35**:561 (1975).
21. A. Zielensny, J. Schmitz, S. Limberg, A. G. Aizpiri, S. Fusenig, and D. Woerman, *Int. J. Thermophys.* **15**:67 (1994).
22. R. Folk and G. Moser, *Condensed Matter Phys. (Ukraine)* **7**:27 (1996); R. Folk and G. Moser, in *Lectures on Cooperative Phenomena in Condensed Matter*, D. I. Uzunov, ed. (Heron Press, Sofia, 1996).
23. J. Pankert and V. Dohm, *Phys. Rev. B* **40**:10842, 10856 (1989).
24. G. Moser, J. Pankert, and V. Dohm, unpublished manuscript.
25. R. Dengler and F. Schwabl, *Z. Phys. B* **69**:327 (1987).
26. R. A. Ferrell, *Int. J. Thermophys.* **10**:369 (1989).
27. D. B. Roe, B. A. Wallace, and H. Meyer, *J. Low Temp. Phys.* **16**:51 (1974).
28. D. B. Roe and H. Meyer, *J. Low Temp. Phys.* **30**:91 (1978).
29. D. Sarid and D. S. Cannell, *Phys. Rev. A* **15**:735 (1977).